PAPER

Check for updates

N,N-Dimethyl-*p*-toluidine crosslinker enables acrylic-based resin with seamless adhesion and high performance

Zhaoquan Qin,[a,d] Huakun Xing,[a,b] Bingbing Wang,[c] Liang Peng,[d] Hai Li [ID] *[a] and Mengjie Long*[c,e]

This study focuses on the development of a novel seamless adhesive by investigating the interaction of *N,N*-dimethyl-*p*-toluidine (DMPT) in an acrylic-based polymer system. The optimal proportions of benzoyl peroxide (BPO) and DMPT were determined to achieve ideal curing time and fracture toughness, making the adhesive highly suitable for industrial applications. The prepared adhesive demonstrated a curing time that balances efficiency with performance, facilitating seamless splicing of artificial stone materials in production lines. The optimal curing time achieved was approximately 10 min at 25 °C, with a stress intensity factor (K) reaching up to 12.32 kPa m$^{1/2}$, demonstrating significant improvement in both efficiency and mechanical strength. Additionally, the ability to adjust the resin-to-powder ratio presents significant cost-saving opportunities for manufacturers. The adhesive exhibited remarkable color stability, with minimal changes observed even under elevated temperatures, resulting in nearly invisible splicing joints. These qualities, combined with strong bonding performance and aesthetic advantages, make the adhesive a promising candidate for use in bioelectronic devices, where durability, versatility, and optical clarity are essential. This research demonstrates the potential of advanced acrylic adhesives to enhance both traditional construction applications and emerging technologies in bioelectronics.

1 Introduction

Seamless splicing refers to a specialized processing technique where the seams between cut pieces of materials are treated to create a visually uninterrupted surface.[1] This process, which involves using advanced adhesives and precise application techniques, not only elevates the aesthetic quality of the installation but also addresses practical concerns, such as preventing dirt and debris from accumulating in the seams. In high-end interior design, where attention to detail is paramount, the ability to create a seamless surface can significantly enhance the perceived value of a project. The success of seamless splicing is heavily dependent on the adhesive used in the process.[2] This adhesive must not only provide strong bonding

but also meet various performance criteria, including resistance to mold, stains, and aging, as well as minimal shrinkage.[3] The importance of these characteristics becomes evident when considering the long-term performance of the installation. For instance, in environments with high humidity, such as bathrooms or kitchens, the mold resistance of the adhesive is crucial in maintaining the integrity and appearance of the surface over time.[4]

Beyond its role in construction and interior design, seamless splicing technology holds significant potential in the field of electronic device adhesion.[5–8] As electronic devices become more compact and multifunctional, adhesives must create strong, reliable bonds between sensitive components while preventing contamination from environmental factors like dust and moisture. In device packaging, especially in consumer electronics, adhesives serve a dual purpose: securing internal components and shielding them from external stressors such as heat, moisture, and mechanical impacts. Seamless adhesion techniques, which form uniform and continuous bonds without visible seams or gaps, are particularly well-suited for encapsulating sensitive electronics.[9,10] These packaging methods not only safeguard the internal components but also contribute to a sleeker, more compact design. Moreover, for layer-to-layer packaging, a crucial com-

[a]Jiangxi Provincial Key Laboratory of Flexible Electronics, Jiangxi Science & Technology Normal University, Nanchang, China. E-mail: lihaiksd@jxstnu.edu.cn
[b]Jiangxi Provincial Key Laboratory of Flexible Electronics, Nanchang Jiaotong Institute, Nanchang, Jiangxi, PR China
[c]Weifang Laksas New Material Technology Co., Ltd, Shandong, China
[d]School of Pharmacy, Jiangxi Science & Technology Normal University, Nanchang, China
[e]Shandong Kelesi New Material Technology Co., Ltd, Shandong, China.
E-mail: longmengjie@sdkelesi.com

ponent in modern electronics such as flexible circuits and multilayer printed circuit boards, adhesives must effectively bond multiple substrate layers without introducing defects or compromising electrical conductivity.[11,12] Seamless adhesive applications play a crucial role in ensuring these layers are securely bonded without gaps, reducing the risk of delamination or failure due to environmental exposure. This type of packaging demands adhesives with high precision, thermal management capabilities, and robust interlayer adhesion, ensuring the reliability and longevity of the electronic devices in which they are used.[13] Seamless splicing achieves visually uninterrupted joints primarily through careful matching of adhesive refractive indices with the substrates, precise control over curing-induced shrinkage, and optimized curing conditions that result in uniform polymer networks. Unlike traditional splicing methods that can leave visible seams due to shrinkage or mismatched refractive indices, seamless splicing techniques utilize advanced adhesives formulated to closely replicate substrate optical properties. This ensures minimal optical distortion and virtually invisible interfaces, which is particularly beneficial in high-end construction and sensitive electronics applications.

Among the adhesives commonly used for seamless splicing, acrylic adhesives, epoxy resin adhesives, and unsaturated resin adhesives are the most prevalent.[14] Acrylic adhesives, in particular, have gained widespread acceptance in the industry due to their superior bonding strength, weather resistance, stain resistance, and resistance to yellowing.[15] These properties make them an ideal choice for both residential and commercial applications, where long-term durability and aesthetics are critical. Acrylic adhesives are formulated using methyl methacrylate (MMA) and polymethyl methacrylate (PMMA) as base materials, along with curing agents and various additives that enable rapid curing at room temperature. This quick curing process not only improves processing efficiency but also enhances the overall outcome by minimizing the time between application and completion. Since only the MMA component shrinks during polymerization and a high polymerisation shrinkage-strain can be reduced by admixing PMMA powder with MMA liquid.[16] The curing systems used in acrylic adhesives are typically classified into cumene hydroperoxide (CHP) and dibenzoyl peroxide (BPO) systems, with the BPO system being the most common due to its effectiveness and reliability in various environmental conditions.[17] Increasing amounts of BPO initiator in the powder and amine in the liquid increased the rate of polymerisation and the magnitude of the exothermic temperature.[18] Acrylic polymer has several advantages such as its good solubility in several solvents, transparency, good adhesive power, and low rigidity of the polymer at room temperature.[19] Polymethyl methacrylate is a thermoplastics can be reused and are transparent.[20] The innovated acrylic solid surfaces have overcome the disadvantages of natural stones such as color staining, water absorption, heavyweight, expensive cost, hard processing and poor resistance to weak acids.[21] In addition, the prepared acrylic solid surface samples represent a cheap and durable replacement to the natural stones. Therefore, the application of seamless stitching acrylic adhesive this technology is particularly important.

Advantages and disadvantages of acrylic adhesive application. To address gaps stemming from thermal expansion coefficient discrepancies between the lead rod and steel plate, melting and pouring lead are avoided. Instead, a construction-oriented approach with adhesive bonding integrates the precision-machined lead rod with the steel plate, ensuring their seamless cooperation.[22] Orthopedic-grade PMMA bone cement, admixed with prophylactic antibiotics, is widely used in hip and knee replacement surgery.[23] Light-curable dental resin-based materials are comprised of methacrylates.[24] However, despite their advantages, acrylic adhesives are not without challenges. One significant issue is their sensitivity to air; MMA can volatilize quickly upon exposure, leading to surface peeling, which compromises the seamless appearance. Additionally, the strong odor of MMA during application can be unpleasant and may require proper ventilation in enclosed spaces.[17] Another challenge is the tendency of acrylic adhesives to yellow after curing, particularly when exposed to sunlight or other ultraviolet (UV) light sources. This yellowing effect can result in noticeable color differences between the surface and the interior, detracting from the desired seamless look.[25] Furthermore, acrylic adhesives exhibit poor stability under extreme temperature conditions, which can limit their application in areas subject to significant temperature fluctuations.[26] The issue of self-polymerization also affects the shelf life of these adhesives, making it necessary to use them within a certain time frame to ensure optimal performance. Finally, in certain cases, such as with black adhesives, there is a problem with incomplete curing, which can lead to reduced bonding strength and aesthetic inconsistencies.[25] To address these challenges, ongoing research and development efforts are focused on improving the formulation of acrylic adhesives. For instance, advances in polymer science have led to the development of new additives that can enhance the UV resistance and color stability of these adhesives.[27] Case studies have shown that the use of UV stabilizers in acrylic adhesives can significantly reduce the yellowing effect, thereby preserving the visual integrity of the seamless splicing over time. Additionally, innovations in adhesive application techniques, such as controlled environment application and the use of vacuum sealing during the curing process, have been explored to mitigate the effects of air sensitivity and improve overall adhesion quality. Moreover, the exploration of alternative adhesive systems, such as hybrid adhesives that combine the properties of acrylics with other resin types, has shown promise in addressing the limitations of traditional acrylic adhesives.[28] These hybrid systems offer enhanced performance in terms of temperature stability, adhesion strength, and curing consistency, making them suitable for a wider range of applications.

Therefore, this study developed a novel seamless adhesive by investigating the interaction of *N,N*-dimethyl-*p*-toluidine (DMPT) on acrylic based resin. The study identified the ideal proportions of benzoyl peroxide (BPO) and DMPT to achieve optimal curing time and fracture toughness. The curing time

of the prepared acrylic adhesive was found to be optimal for industrial production lines, offering a balance between efficiency and performance. Moreover, adjusting the ratio of polymer to powder has the potential to reduce costs and increase profitability for manufacturers. The color stability of the acrylic adhesives was also remarkable, with minimal changes observed even at elevated temperatures, ensuring a superior seamless splicing effect with virtually no visible traces.[29] Over time, the adhesives exhibit excellent resistance to yellowing and aging, maintaining a bright and transparent appearance compared to other splicing agents available in the market. These characteristics make the adhesive promising for use in bioelectronic devices, where material durability, flexibility, and optical clarity are critical.[5,6,8,30–35]

2 Experimental section

2.1 Materials

Polymethyl methacrylate (PMMA) and methacrylate (MMA) were provided by J&K Scientific (Beijing, China). Defoamer 555 was purchased from BASF SE (Guangzhou, China). Trimethylolpropane trimethacrylate (TMPTA), 3-ethacryloxy-propyltrimethoxysilane, tetramethylthiourea, *N,N*-dimethyl-*p*-toluidine (DMPT), *N,N*-dimethylacrylamide (DMA) and dipropylene glycol methyl ether (DPE) were obtained from Aladdin Co., Ltd (Shanghai, China). Benzoyl peroxide (BPO) and epoxy resin were sourced from Xingchen Synthetic Materials Co., Ltd (Nantong, China). All other reagents were of analytical grade and used as received without further purification.

2.2 The preparation of the seamless adhesive

The production process of reagent A is as follows: 50 g of PMMA pellets are dissolved in 50 g of MMA solution. Subsequently, 10 g of methacrylic acid, 5 g of tetramethyl-thiourea, 3 g of coupling agent 3-ethacryloxypropyl-trimethoxysilane, 3 g of cross-linker TMPTA and an appropriate amount of DMPT are added. The mixture is stirred at 1000 rpm for 10 min and then allowed to stand to remove bubbles. Finally, reagent A is mixed with reagent B in a 10:1 ratio to prepare the seamless adhesive.

The production process for reagent B is as follows: 5.5 g of BPO paste and 3 g of high-boiling solvent DPE are mixed at 500 rpm for 2 min. Gradually, 94.5 g of epoxy resin is added and stirred at the same speed until uniform. Then, 0.005 g of defoamer 555 are added, with continued stirring for 10 min. The mixture is filtered through an 80-mesh screen and left to rest for 2 h to remove any bubbles, ensuring product consistency.

The curing time measurement was determined by monitoring the exothermic reaction during adhesive curing. Specifically, the adhesive surface temperature was measured using an infrared detector, and temperature data were recorded every 30 s. The curing time was identified as the point at which the adhesive reached its peak exothermic temperature, indicating completion of the curing process (Fig. 1 and 2).

2.3 Fracture toughness measurement

The fracture toughness of the specimens was measured using a DKZ-5000 anti-rupture testing machine equipped with a three-point bending device. The stress intensity factor of the artificial stone, bonded with acrylic adhesive, was evaluated using stan-
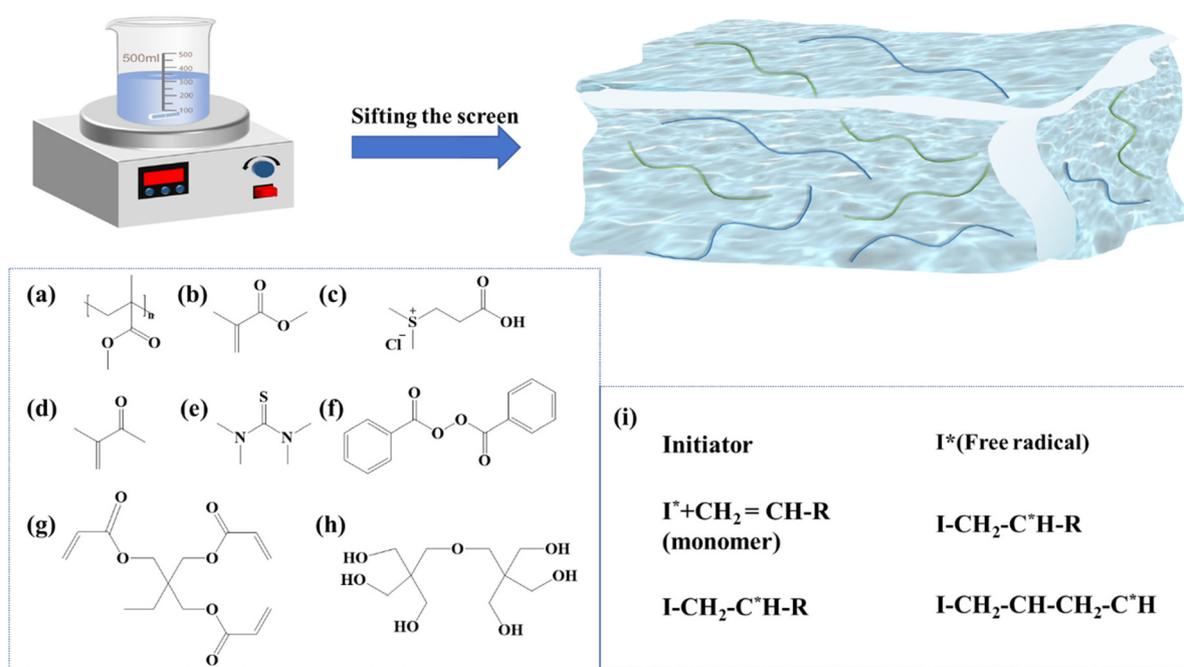

Fig. 1 Acrylic adhesive preparation process. (a) PMMA. (b) MMA. (c) DMPT. (d) Methacrylic acid. (e) Tetramethylthiourea. (f) BPO. (g) TMPTA. (h) DPE. (i) Mechanism of crosslinking agent.
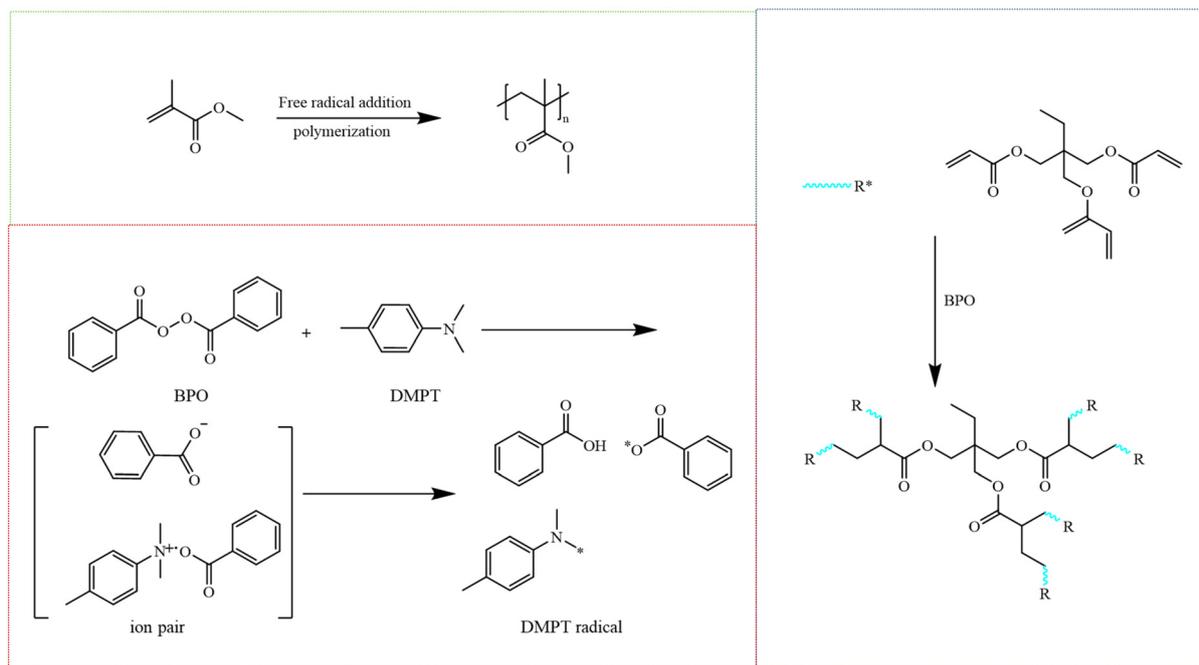
© 2025 The Author(s). Published by the Royal Society of Chemistry

RSC Appl. Polym., 2025, **3**, 855–864 | **857**

Fig. 2 Schematic illustration showing the free-radical polymerization of MMA, as initiated by BPO-DMPT and the synthesis of poly(methyl methacrylate) PMMA by free radical addition polymerization of methyl methacrylate MMA.[36–39]

dard specimens measuring 40 mm × 40 mm × 160 mm. The parameters of the DKZ-5000 testing machine are provided in Fig. 3a, while Fig. 3b illustrates the schematic diagram of the fracture toughness testing setup. During testing, load-displacement curves were recorded, and the mode-I stress intensity factor (K) was calculated using the following equation:

$$K = \frac{3PL}{2BW^{3/2}}f\left(\frac{a}{W}\right)$$

where P is the maximum load at fracture, L is the span length between supports, B is the specimen thickness, W is the specimen width, and a is the initial crack length. The geometric factor $f(a/W)$ accounts for specimen geometry and crack length.

2.4 Determination of color

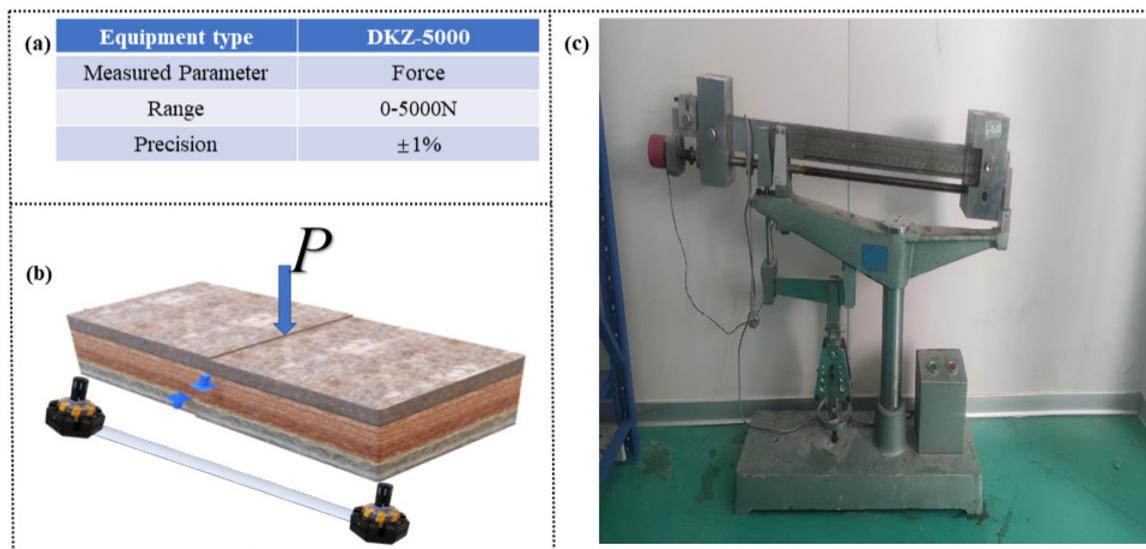The color of the acrylic adhesives was determined using an NR-200 Chroma Meter (3nh Technology Co., Ltd, Shenzhen,

Fig. 3 Test equipment and mechanism. (a) Parameters of DKZ-5000. (b) Schematic diagram of fracture toughness. (c) DKZ-5000.

858 | *RSC Appl. Polym.*, 2025, **3**, 855–864

© 2025 The Author(s). Published by the Royal Society of Chemistry

China). Prior to measurement, the chroma meter was calibrated using black and white reference standards. The color information was quantified based on the *Lab** color space, where *L* represents brightness, *a* indicates the shift from green (−) to red (+), and *b* reflects the shift from blue (−) to yellow (+).

3 Results and discussion

3.1 Effect of curing time and fracture toughness

3.1.1 Effects of DMPT content on curing time and stress intensity factor.
Fig. 4 illustrates the effect of DMPT content (0.3 g, 0.5 g, and 0.7 g) on curing time and stress intensity factor under mode-I loading. As the BPO content increases from 3.5 to 4.5 and 5.5, stress intensity factor shows a positive correlation, gradually increasing with higher BPO content. It is also evident from the figure that the curing time decreases as the DMPT content increases. Specifically, with DMPT contents of 0.3 g, 0.5 g, and 0.7 g, the curing time decreases by 16, 14, and 10 min, respectively. Additionally, as the DMPT content increases, the stress intensity factor rises approximately linearly. The reduction in stress intensity factor with shorter curing times is likely related to the enhancement of bonding strength facilitated by the increasing BPO content.

The observed relationship between DMPT content, BPO content, curing time, and stress intensity factor can be explained by the roles these components play in the polymerization process. DMPT acts as an accelerator, enhancing the rate of the redox reaction between the initiator (BPO) and the monomers in the adhesive. As the DMPT content increases, the initiation of polymerization is accelerated, leading to a shorter curing time. This is because DMPT facilitates the decomposition of BPO, which in turn generates more free radicals that initiate the polymerization process more quickly.

In terms of stress intensity factor, an increase in BPO content promotes the generation of cross-linked polymer chains, which improves the mechanical strength of the adhesive. This cross-linking leads to a more robust and cohesive network structure, which enhances the adhesive's ability to resist crack propagation, resulting in higher stress intensity factor. However, if the curing time becomes too short, there might not be sufficient time for the polymer network to fully develop, which could limit the enhancement in mechanical properties. Therefore, the balance between curing time and stress intensity factor is critical, as both depend on the interactions between DMPT and BPO in driving the polymerization process.

3.1.2 Effect of different ratio of resin and powder on curing time and fracture toughness.
As shown in Fig. 5, stress intensity factor and curing time were tested for artificial stone samples with different resin-to-powder ratios of 10 : 0, 7 : 3, 6 : 4, 5 : 5, and 4 : 6 (weight ratio). The decrease in curing time and stress intensity factor with increasing aluminum hydroxide content can be attributed to the role of aluminum hydroxide in the adhesive matrix. Aluminum hydroxide serves as a filler material in the binder, and as its content increases, it dilutes the concentration of reactive polymer components in the adhesive. This dilution slows down the cross-linking process during curing, resulting in a shorter curing time. Furthermore, the increased filler content may also disrupt the formation of a uniform, cohesive polymer network, leading to reduced mechanical properties such as stress intensity factor. The presence of excessive filler particles can create weak points in the adhesive, where stress is concentrated during loading, making the material more susceptible to cracking. However, the inclusion of aluminum hydroxide is advantageous for cost reduction in industrial production, as it reduces the amount of more expensive polymer materials needed without significantly compromising the adhesive's performance. In industrial applications, optimizing the resin-to-powder ratio is essential to strike a balance between performance and production efficiency. A curing time of less than 14 min ensures faster production cycles, while maintaining stress intensity factor above the required threshold guarantees the final product's reliability and durability.

In order to illustrate the practical applicability and performance superiority of our developed seamless bonding adhesive under realistic conditions, a comparative bonding experiment was conducted using two artificial stone slabs, each measuring 4 × 5 cm. The long edges of these slabs were first precisely cut at a 45-degree angle to simulate common joint interfaces encountered in practical applications. Subsequently, one pair of slabs was bonded using a conventional single-component silicone rubber adhesive, while another pair was bonded with our newly developed adhesive (resin-to-powder ratios is 10 : 0,
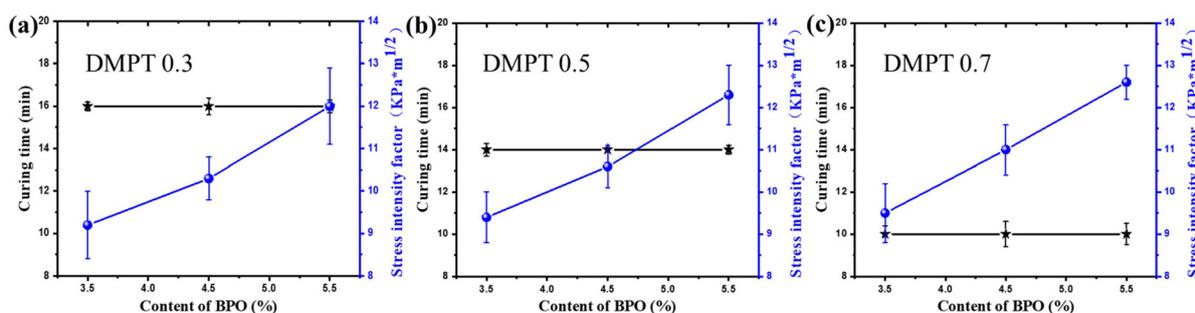

Fig. 4 The evolution of mode-I curing time and stress intensity factor of DMPT of a content of 0.3 g, 0.5 g and 0.7 g. (a) 0.3 g DMPT. (b) 0.5 g DMPT. (c) 0.7 g DMPT.
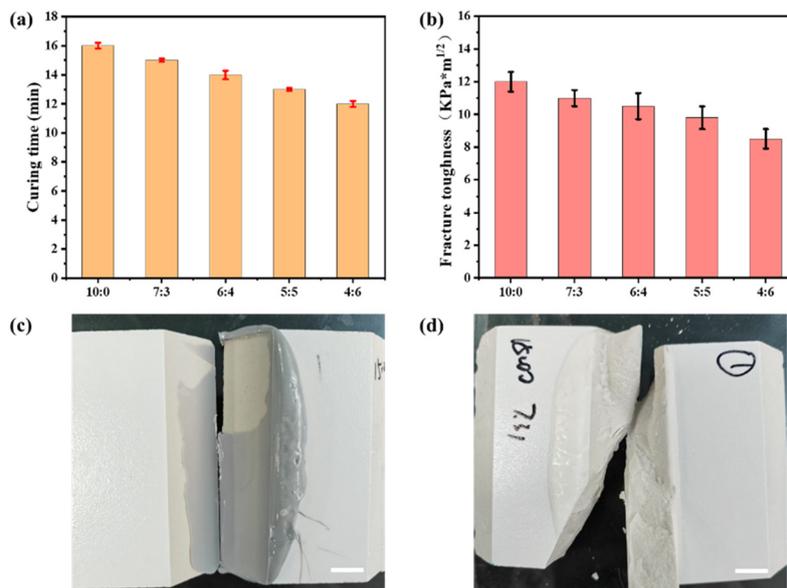
Fig. 5 Effect of different weight ratio of resin and powder on curing time and stress intensity factor. (a) Effect on curing time. (b) Effect on curing time. (c) Photo of the splicing effect of traditional single component silicone rubber adhesive. (d) Photo of the splicing effect of our seamless splicing acrylic adhesive. Scare bar is 2 cm.

DMPT is 0.7). After bonding, the samples were allowed to cure undisturbed for two hours to ensure adequate adhesive hardening. Following the curing period, the bonded slabs were subjected to a manual fracture test involving deliberate forceful impacts. The fracture surfaces were then carefully examined for residual adhesive. The results indicated a distinct difference: significant visible adhesive residue remained on the fractured surfaces of the slabs bonded with the conventional silicone rubber adhesive (Fig. 5c), highlighting adhesive rather than substrate failure. In contrast, the slabs bonded using our adhesive exhibited clean fracture surfaces, completely free from visible adhesive residues (Fig. 5d). This clearly demonstrates that the fracture mode of our adhesive was cohesive within the substrate rather than adhesive failure at the bonding interface, signifying stronger adhesion and seamless integration between substrates.

3.1.3 Effect of different temperature on curing time. From the Table 1, it is evident that when the DMPT content remains constant at a given curing temperature, the curing time shows minimal change as the BPO content gradually increases. However, when the curing temperature remains the same and the BPO content is held constant, the curing time decreases significantly with increasing DMPT content. Additionally, for the same ratio of acrylic adhesives, the curing time is reduced considerably as the curing temperature increases. The observed effects of temperature and DMPT content on curing time can be attributed to the chemical kinetics of the polymerization process. At higher temperatures, the reaction rate of the polymerization process increases due to enhanced molecular movement and more frequent collisions between reactive species. This leads to faster initiation and propagation of the polymer chains, significantly reducing the curing time. DMPT

Table 1 High and low temperature activity of acrylic adhesives in different proportions

		Curing temperature (°C)		
		5	25	40
DMPT (g)	BPO (g)	Curing time (min)		
0.3	3.5	35	16	12
0.3	4.5	35	16	12
0.3	5.5	35	16	12
0.5	3.5	28	14	10
0.5	4.5	28	15	10
0.5	5.5	28	14	10
0.7	3.5	20	10	8
0.7	4.5	20	10	8
0.7	5.5	20	10	8

acts as an accelerator, facilitating the decomposition of BPO to generate free radicals that drive the polymerization process. When the DMPT content increases, more free radicals are generated in a shorter time, further accelerating the curing process. This explains why, at a constant temperature, an increase in DMPT content leads to a noticeable reduction in curing time, even when the BPO content remains unchanged. Overall, higher temperatures and increased DMPT content both contribute to faster polymerization, reducing the curing time and making the adhesive more suitable for industrial applications requiring rapid processing.

3.2 Effect of different acrylic adhesives on the changes in color

3.2.1 Effect of temperature on the change of color with the different additives. The positive value of L indicates that the

RSC Applied Polymers

Paper

solution is bright, the negative value of *a* indicates that the solution is greenish, and the positive value of *b* indicates that the solution is yellowish. ΔE is a single value that combines changes in *L* (lightness), *a* (green to red), and *b* (blue to yellow) to quantify the total color difference between two samples. It is calculated using the formula: $\Delta E = [(\Delta L)^2 + (\Delta a)^2 + (\Delta b)^2]^{1/2}$. By utilizing ΔE, we can objectively quantify the perceptible color differences resulting from temperature variations, offering a more comprehensive understanding of the color stability of the adhesives. This approach ensures that our analysis is both scientifically robust and perceptually relevant. The variation of components *N,N*-dimethyl-*p*-toluidine (DMPT) and *N,N*-dimethylacrylamide (DMA) with temperature on color in acrylic adhesives. As shown in Fig. 5, it was observed that the temperature of the DMA takes 20 min to rise from normal temperature to 135 degrees celsius, *L* value decreased from 95.15 to 94.48, *b* increased from 2.65 to 3.50, and an increased from −0.11 to −0.08 as the temperature values increased. The value of ΔE is 0.86. As shown in Table 2, the temperature of the DMA takes 30 min to rise from normal temperature to 165 degrees celsius, *L* value decreased from 95.49 to 95.44, *b*

increased from 1.96 to 3.05, and an increased from −0.30 to −0.14 as the temperature values increased. The value of ΔE is 1.09. The changes in color with increasing temperature can be explained by the thermal effects on the chemical structure of the components in the acrylic adhesives. As the temperature increases, molecular changes in DMPT and DMA, such as the interaction between functional groups, can lead to variations in their light absorption and reflection properties. This results in shifts in color values, particularly in the brightness (*L*), green-red balance (*a*), and blue-yellow balance (*b*).

The temperature of the DMPT takes 20 min to rise from normal temperature to 135 degrees celsius, *L* value increased from 95.56 to 95.59, *b* increased from 0.59 to 1.03, and *a* decreased from −0.23 to −0.36 as the temperature values increased. The value of ΔE is 0.46. As shown in Table 2, the temperature of the DMPT takes 30 min to rise from normal temperature to 165 degrees celsius, *L* value decreased from 95.77 to 95.57, *b* increased from 0.40 to 0.98, and *a* decreased from −0.12 to −0.46 as the temperature values increased. The value of ΔE is 0.71. The components DMA in acrylic adhesives become lighter green as the temperature rises. As the temperature rises, the component DMPT green color in acrylic adhesives deepens. The yellow color of the components DMPT and DMA in acrylic adhesives deepens as the temperature rises. In the case of DMA, the slight darkening and increasing yellow tint with rising temperature suggest that the material undergoes thermal degradation or oxidation, which leads to the production of chromophores that reflect more yellow light. For DMPT, the deepening of the green hue as the temperature rises may be linked to structural changes that enhance the absorption of red light, thus making the material appear greener. The observed color changes at elevated temperatures may be attributed to thermal-induced oxidation or structural alterations in the DMPT molecules. Under increased temperature, oxidation reactions or slight molecular rearrangements of

Table 2 Effect of temperature on the color of the different ingredients in acrylic adhesives

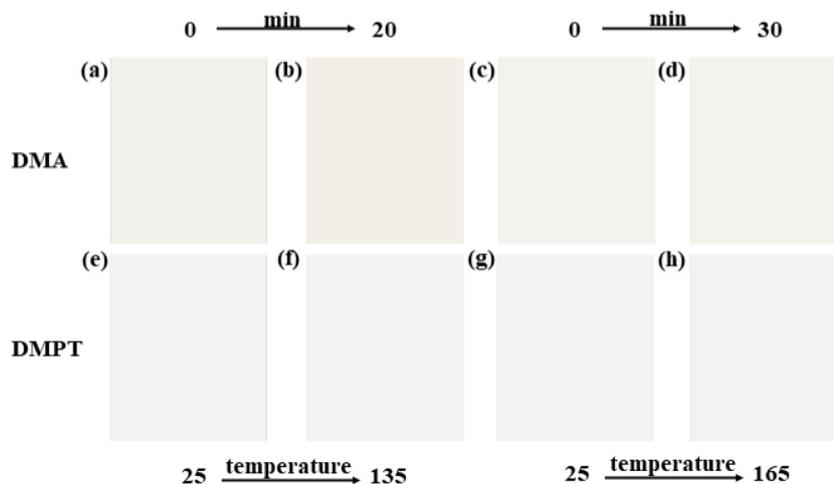|	Temperature(°C)	Time(min)	*L*	*a*	*b*	ΔE
DMA	25	0	95.15	−0.11	2.65	0.86
	135	20	94.48	−0.08	3.50	
	25	0	95.49	−0.30	1.96	1.09
	165	30	95.44	−0.14	3.05	
DMPT	25	0	95.56	−0.23	0.59	0.46
	135	20	95.59	−0.36	1.03	
	25	0	95.77	−0.12	0.40	0.71
	165	30	95.57	−0.46	0.98	

Fig. 6 The variation of components DMPT and DMA with temperature on color in acrylic adhesives. (a) and (c) The color of DMA at 25 degrees celsius. (b) The color of DMA at 135 degrees celsius. (d) The color of DMA at 165 degrees celsius. (e) and (g) The color of DMPT at 25 degrees celsius. (f) The color of DMPT at 135 degrees celsius. (h) The color of DMPT at 165 degrees celsius.

Paper

RSC Applied Polymers

DMPT could generate chromophoric groups, thereby affecting the color stability and optical properties of the adhesive. The overall changes in color difference (ΔE) provide a quantitative measure of the extent of these shifts, which are relatively small, indicating that the adhesives maintain color stability within the tested temperature range (Fig. 6).
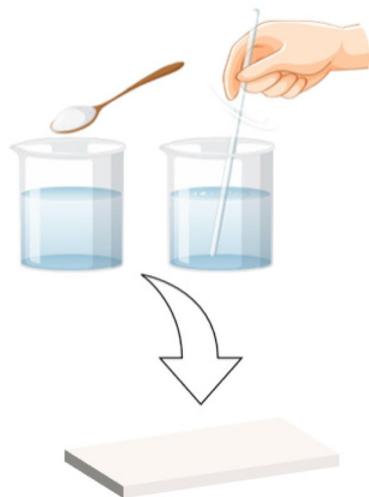

Fig. 7 Different types of ultraviolet absorbers added to acrylic adhesive different color difference performance. (a) Blank, the value of ΔE is 4.55. (b) Basf 329 UV absorber was added, the value of ΔE is 24.39. (c) Basf 326 UV absorbent was added, the value of ΔE is 23.63. (d) Added Chick 2912 UV absorber, the value of ΔE is 5.28.
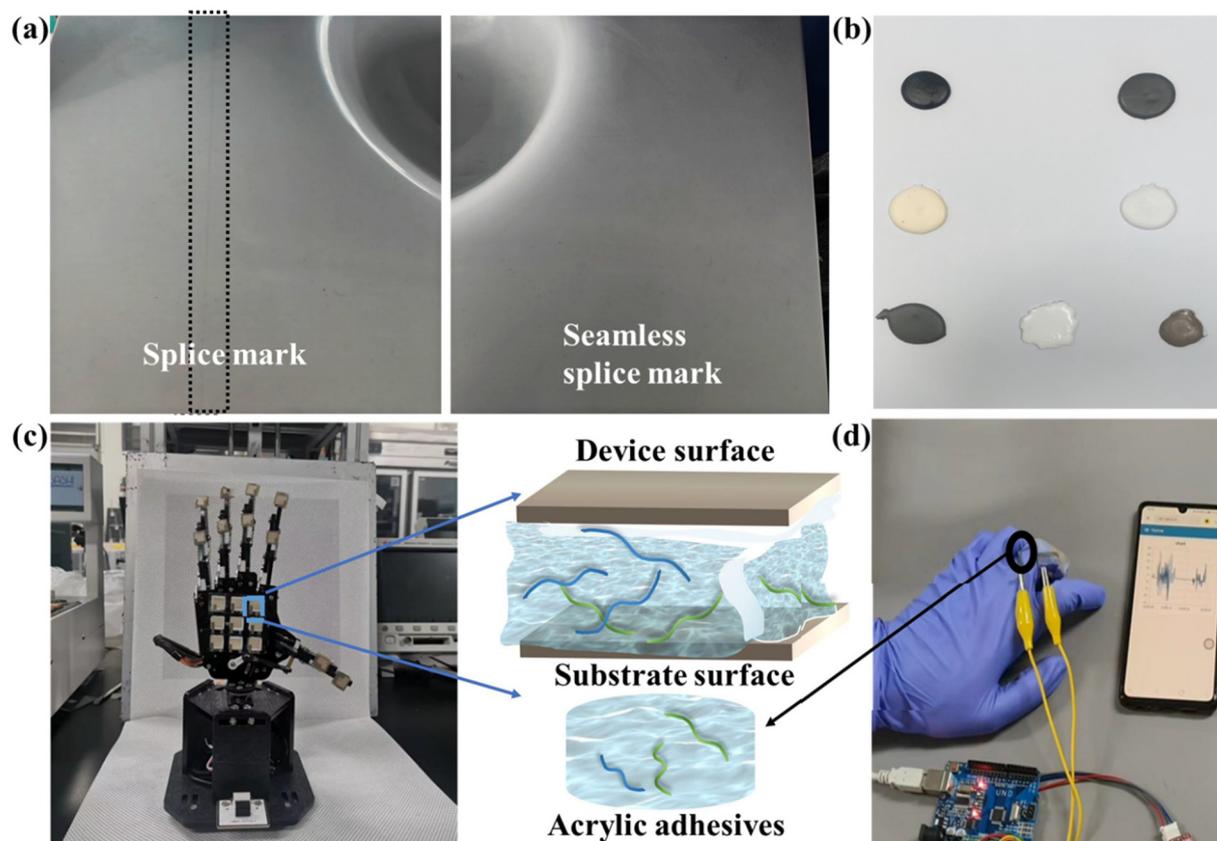

Fig. 8 The advantages of acrylic adhesives over other splicing adhesives. (a) The application of adhesive for seamless splicing. (b) The color of adhesive. (c) The application of adhesive for device adhesion on robot hand. (d) The application of adhesive for biodevice adhesive on human hand.

862 | *RSC Appl. Polym.*, 2025, **3**, 855–864

© 2025 The Author(s). Published by the Royal Society of Chemistry

3.2.2 The effect of UV absorbent on the changes of color. UV radiation can cause degradation in polymers, leading to discoloration, most notably yellowing, which compromises the aesthetic quality of materials like acrylic adhesives. The addition of UV absorbers helps to block or absorb harmful UV rays, preventing them from reaching the adhesive's polymer matrix and causing degradation. By preventing these chemical changes, the UV stabilizers reduce the yellowing effect, ensuring that the adhesive remains visually consistent over time. Ultraviolet radiation can cause photodegradation and photooxidative degradation by breaking chemical bonds within polymers, leading to discoloration and reduced performance. Therefore, we selected three representative ultraviolet absorbers (Chick 2912, Basf 329 UV, and Basf 326 UV) due to their proven effectiveness reported in prior research.[40,41] Specifically, Basf 326 UV was previously demonstrated to have superior UV absorption capability compared to other common industrial absorbers such as Irgafos 168, Irganox 1010, and UV-531, effectively absorbing wavelengths from 290 to 420 nm. Additionally, benzotriazole-based UV absorbers like Chick 2912 were chosen based on their documented success in achieving excellent UV stability and transparency through integration into polymer matrices *via in situ* polymerization methods. Thus, these absorbers were selected for comparative analysis due to their established performance and relevance to our application. As shown in Fig. 7, different UV absorbers have varying effectiveness, with the best-performing stabilizer (Fig. 7d) showing the smallest color difference. This indicates that the adhesive with this absorber maintains its color stability the most effectively, which is critical for applications where long-term appearance is essential, such as seamless stitching.

3.2.3 The applications of acrylic adhesives. Acrylic adhesives have found widespread applications due to their versatile properties, particularly in the construction of artificial stone and other composite materials. As demonstrated in Fig. 8a, our acrylic adhesives exhibit significant advantages over conventional splicing adhesives, producing nearly seamless joints with no visible traces, resulting in a smooth and aesthetically pleasing surface. A key step in our experimental process involved incorporating various color pigments into the prepared water-based coatings. We successfully formulated coatings in seven distinct colors as shown in Fig. 8b. This versatility in color mixing provides a robust foundation for further applications, where color variety and consistency are critical. The successful integration of diverse pigments into our coatings not only expands the potential application range but also demonstrates the practical adaptability of our formulations for various industrial uses. Furthermore, the prepared adhesives were tested for adhesion in electronic devices, demonstrating excellent bonding performance, as shown in Fig. 8c and d. The strong adhesion properties make these adhesives particularly well-suited for use in sensitive electronic applications, where secure and durable bonding is critical to maintaining device integrity over time. This includes applications in wearable electronics, flexible circuits, and bioelectronic sensors, where adhesives must withstand mechanical stress, environmental factors, and thermal fluctuations without compromising performance.

4 Conclusions

This study successfully developed a novel seamless adhesive by investigating the interaction of *N,N*-dimethyl-*p*-toluidine (DMPT) within an acrylic-based polymer system. The ideal proportions of benzoyl peroxide (BPO) and DMPT were identified to achieve optimal curing time and fracture toughness, making the adhesive particularly suitable for industrial applications. The adhesive demonstrated a well-balanced curing time that enhances both processing efficiency and performance, facilitating seamless splicing of artificial stone in production environments. Additionally, adjusting the polymer-to-powder ratio provides significant cost-saving potential for manufacturers. The adhesive exhibited exceptional color stability, with minimal changes under elevated temperatures, ensuring nearly invisible splicing joints. Its long-term durability was supported by outstanding resistance to yellowing and aging, maintaining a bright and transparent appearance over time. These combined characteristics, such as strong bonding performance, durability, and aesthetic appeal, position this adhesive as a promising candidate for bioelectronic devices, where durability, versatility, and optical clarity are critical. This research highlights the potential for advanced acrylic adhesives to enhance both traditional construction practices and emerging technologies in bioelectronics.

Data availability

The data that support the findings of this study are available from the corresponding author, upon reasonable request.

Conflicts of interest

The authors declare that they have no known competing financial interests or personal relationships that could have appeared to influence the work reported in this paper.

Acknowledgements

References

1 A. T. Wolf and A. Stammer, *Polymers*, 2024, **16**, 2220.
2 R. Avendaño, R. Carbas, E. Marques, L. F. da Silva and A. Fernandes, *Compos. Struct.*, 2016, **152**, 34–44.

© 2025 The Author(s). Published by the Royal Society of Chemistry

RSC Appl. Polym., 2025, **3**, 855–864 | **863**

3 S. R. Mousavi, S. Estaji, M. R. Javidi, A. Paydayesh, H. A. Khonakdar, E. Rostami and S. H. Jafari, *J. Mater. Sci.*, 2021, **56**, 18345–18367.

4 C. S. Borges, A. Akhavan-Safar, P. Tsokanas, R. J. Carbas, E. A. Marques and L. F. da Silva, *Discover Mech. Eng.*, 2023, **2**, 8.

5 J. Yu, R. Wan, F. Tian, J. Cao, W. Wang, Q. Liu, H. Yang, J. Liu, X. Liu, T. Lin, J. Xu and B. Lu, *Small*, 2024, **20**, 2308778.

6 J. Yu, F. Tian, W. Wang, R. Wan, J. Cao, C. Chen, D. Zhao, J. Liu, J. Zhong, F. Wang, Q. Liu, J. Xu and B. Lu, *Chem. Mater.*, 2023, **35**, 5936–5944.

7 R. Wan, J. Yu, Z. Quan, H. Ma, J. Li, F. Tian, W. Wang, Y. Sun, J. Liu, D. Gao, J. Xu and B. Lu, *Chem. Eng. J.*, 2024, **490**, 151454.

8 Z. Zhang, G. Chen, Y. Xue, Q. Duan, X. Liang, T. Lin, Z. Wu, Y. Tan, Q. Zhao, W. Zheng, L. Wang, F. Wang, X. Luo, J. Xu, J. Liu and B. Lu, *Adv. Funct. Mater.*, 2023, **33**, 2305705.

9 Z. Wu, Q. Zhao, X. Luo, H. Ma, W. Zheng, J. Yu, Z. Zhang, K. Zhang, K. Qu, R. Yang, N. Jian, J. Hou, X. Liu, J. Xu and B. Lu, *Chem. Mater.*, 2022, **34**, 9923–9933.

10 X. Luo, R. Wan, Z. Zhang, M. Song, L. Yan, J. Xu, H. Yang and B. Lu, *Adv. Sci.*, 2024, 2404679.

11 J. Li, J. Cao, B. Lu and G. Gu, *Nat. Rev. Mater.*, 2023, **8**, 604–622.

12 F. Wang, Y. Xue, X. Chen, P. Zhang, L. Shan, Q. Duan, J. Xing, Y. Lan, B. Lu and J. Liu, *Adv. Funct. Mater.*, 2024, **34**, 2314471.

13 Y. Park, J. Kim, D. Kim, S. Lee, D. Hwang and M. S. Kwon, *Soft Sci.*, 2024, **4**, 28.

14 C. Gao, F. Wang, X. Hu and M. Zhang, *Polymers*, 2023, **15**, 2727.

15 K. Pojnar, B. Pilch-Pitera and R. Patil, *Polimery*, 2024, **69**, 143–158.

16 N. Silikas, A. Al-Kheraif and D. C. Watts, *Biomaterials*, 2005, **26**, 197–204.

17 B. A. Suslick, J. Hemmer, B. R. Groce, K. J. Stawiasz, P. H. Geubelle, G. Malucelli, A. Mariani, J. S. Moore, J. A. Pojman and N. R. Sottos, *Chem. Rev.*, 2023, **123**, 3237–3298.

18 E. E. Rose, J. Lal and R. Green, *J. Am. Dent. Assoc.*, 1958, **56**, 375–381.

19 M. Khallaf, A. El-Midany and S. El-Mofty, *Prog. Org. Coat.*, 2011, **72**, 592–598.

20 Z. He, P. Cheng, G. Ying and Z. Ou, *Appl. Sci.*, 2024, **14**, 6780.

21 H. Mori and A. H. Müller, *Prog. Polym. Sci.*, 2003, **28**, 1403–1439.

22 M. Jia, Y. Chen and P. Jin, *Thin-Walled Struct.*, 2024, **199**, 111822.

23 W. Wei, E. Abdullayev, A. Hollister, D. Mills and Y. M. Lvov, *Macromol. Mater. Eng.*, 2012, **297**, 645–653.

24 F. W. Degrazia, V. C. B. Leitune, A. S. Takimi, F. M. Collares and S. Sauro, *Dent. Mater.*, 2016, **32**, 1133–1143.

25 Y. Zou, Y. Xia and X. Yan, *Polymers*, 2024, **16**, 2308.

26 L. B. Morgado, M. D. S. Pedrosa and I. S. Medeiros, *Oper. Dent.*, 2024, **49**, 76–83.

27 J. Miklečić, M. Zeljko, S. Lučić Blagojević and V. Jirouš-Rajković, *Polymers*, 2024, **16**, 511.

28 J. Lee, H. Lee and G. Kwak, *Small*, 2024, 2404907.

29 R. Bagheri, B. Marouf and R. Pearson, *J. Macromol. Sci., Part C: Polym. Rev.*, 2009, **49**, 201–225.

30 F. Dai, Q. Geng, T. Hua, X. Sheng and L. Yin, *Soft Sci.*, 2023, **3**, 7.

31 A. C. Da Silva and I. R. Minev, *Soft Sci.*, 2023, **3**, 3.

32 G. Li and C. F. Guo, *Soft Sci.*, 2022, **2**, 7.

33 G. Tang, D. Mei, X. Zhao, C. Zhao, L. Li and Y. Wang, *Soft Sci.*, 2023, **3**, 9.

34 B. Lu, H. Yuk, S. Lin, N. Jian, K. Qu, J. Xu and X. Zhao, *Nat. Commun.*, 2019, **10**, 1043.

35 F. Tian, J. Yu, W. Wang, D. Zhao, J. Cao, Q. Zhao, F. Wang, H. Yang, Z. Wu, J. Xu and B. Lu, *J. Colloid Interface Sci.*, 2023, **638**, 339–348.

36 Z. Yan, S. Wang, J. Bi, Q. He, H. Song, I. H. Ei Azab, S. M. Ei-Bahy, A. Y. Elnaggar, M. Huang, M. H. Mahmoud, J. Wang and Q. Shao, *Adv. Compos. Hybrid Mater.*, 2022, **5**, 2116–2130.

37 P. Riggs, M. Braden and M. Patel, *Biomaterials*, 2000, **21**, 345–351.

38 Y.-F. Peng, A. Tsai and M.-H. Huang, *Polym. J.*, 2018, **50**, 967–974.

39 A. F. Elerian, A. A. Mohamed, E. M. Elnaggar, G. Abdel-Naeem and M. A. Abu-Saied, *Polym. Bull.*, 2024, 1–36.

40 T. Jiang, Z. Mao, Y. Qi, Y. Wu and J. Zhang, *Polym. Adv. Technol.*, 2021, **32**(49), 15–4925.

41 G. Huang, C. Yao, M. Huang, J. Zhou, X. Hao, X. Ma, S. He, H. Liu, W. Liu and C. Zhu, *ACS Appl. Mater. Interfaces*, 2023, **15**, 18300–18310.